

# No magnesium is needed for binding of the stimulator of interferon genes to cyclic dinucleotides

Miroslav Smola,<sup>a</sup> Gabriel Birkus<sup>a</sup> and Evzen Boura<sup>a,b\*</sup>

<sup>a</sup>Gilead Sciences Research Centre at IOCB Prague, Institute of Organic Chemistry and Biochemistry of the Czech Academy of Sciences, Flemingovo nam. 2, 166 10 Prague, Czech Republic, and <sup>b</sup>Department of Biochemistry, Institute of Organic Chemistry and Biochemistry, Flemingovo nam. 2, 166 10 Prague, Czech Republic. \*Correspondence e-mail: boura@uochb.cas.cz

Received 9 July 2019  
Accepted 6 August 2019

Edited by P. Dunten, Stanford Synchrotron Radiation Lightsource, USA

**Keywords:** STING; cGAS; CDN; 3',3'-c-di-GMP; crystal structure.

**PDB reference:** STING in complex with 3',3'-c-di-GMP, 6s86

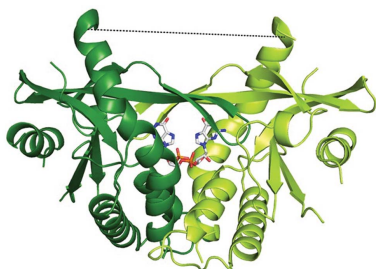
**Supporting information:** this article has supporting information at journals.iucr.org/f

Stimulator of interferon genes (STING) binds cyclic dinucleotides (CDNs), which induce a large conformational change of the protein. The structural basis of activation of STING by CDNs is rather well understood. Unliganded STING forms an open dimer that undergoes a large conformational change ( $\sim 10$  Å) to a closed conformation upon the binding of a CDN molecule. This event activates downstream effectors of STING and subsequently leads to activation of the type 1 interferon response. However, a previously solved structure of STING with 3',3'-c-di-GMP shows Mg atoms mediating the interaction of STING with this CDN. Here, it is shown that no Mg atoms are needed for this interaction; in fact, magnesium can in some cases obstruct the binding of a CDN to STING.

## 1. Introduction

A major marker of intracellular infection by a pathogen is the presence of double-stranded DNA (dsDNA) in the cytoplasm. There it is sensed by the cyclic GMP-AMP (cGAMP) synthase (cGAS), which in turn starts the synthesis of the second messenger 2',3'-cyclic GMP-AMP (cGAMP). cGAMP and other cyclic dinucleotides (CDNs) bind to and activate the stimulator of interferon genes (STING), which is the axis of the cGAS–STING pathway (Chen *et al.*, 2016). Upon activation, STING recruits the kinase TBK1, which phosphorylates the transcription factor IRF3, thus promoting IRF3 dimerization and the transcription of interferons and inflammatory cytokines (Fitzgerald *et al.*, 2003). Notably, overactivation of the cGAS–STING pathway may lead to autoinflammatory diseases such as Aicardi–Goutieres syndrome (Barber, 2015; Strzyz, 2019). The cGAS–STING pathway also plays an important role in tumour surveillance (Barber, 2015), and STING agonists have been shown to exert potent antitumor activity (Corrales *et al.*, 2015; Fu *et al.*, 2015).

STING is an ER-resident 379-amino-acid protein that consists of an N-terminal transmembrane domain and a C-terminal ligand-binding domain that is responsible for its dimerization. The activation of STING by CDNs is relatively well understood. Unliganded STING is a dimer with an open conformation (Shu *et al.*, 2012). Upon binding a CDN the C-terminal ligand-binding domain dramatically shifts by  $\sim 10$  Å to a closed conformation (Fig. 1). Additionally, it has been shown by cryo-EM that cGAMP binding induces the tetramerization of STING, which leads to the transphosphorylation of STING by TBK1 (TBK1 bound to one STING



dimer phosphorylates the other STING dimer) and the subsequent recruitment of the transcription factor IRF3 (Shang *et al.*, 2019). High-order oligomer formation between STING and TBK1 upon cGAMP binding has been proposed as a structural mechanism for the phosphorylation of IRF3 by TBK1 in another cryo-EM study (Zhang *et al.*, 2019).

Activation of STING by CDNs is still not fully understood despite the structural advances mentioned above. Notably, one of the first X-ray structures of STING (PDB entry 4f5d; Huang *et al.*, 2012) has Mg atoms in the active site, while other structures do not (PDB entries 4ksy, 4f9g and 5bqx; Zhang *et al.*, 2013; Yin *et al.*, 2012; Shi *et al.*, 2015). This discrepancy could be caused by the low resolution of some of the structures, as small ligands such as smaller atoms or water molecules are usually not modelled at low resolution, or by misinterpretation of the electron-density maps. Here, we provide biophysical and structural evidence that STING does not bind to CDNs via Mg atoms. We show that a high concentration of magnesium in fact destabilizes CDN–STING complexes and that the best crystals of a CDN–STING complex can be grown using EDTA as an additive in the crystallization trials.

## 2. Materials and methods

### 2.1. Protein expression and purification

A DNA sequence encoding the cytosolic domain of human STING (residues 140–343) was inserted into pHis2 vector with an N-terminal 8×His-SUMO solubility tag by restriction cloning. The protein was expressed and purified according to standard protocols (Hercik *et al.*, 2017; Boura *et al.*, 2010). Briefly, the protein was expressed in the *Escherichia coli* BL21 (DE3) NiCo bacterial strain using ZY5052 autoinduction medium. The cells were grown at 310 K until they reached an OD<sub>600</sub> of 1. The temperature was then decreased to 291 K and the cells were cultivated overnight. The cells were harvested and were lysed in lysis buffer (300 mM NaCl, 50 mM Tris pH 8, 30 mM imidazole, 3 mM β-mercaptoethanol, 10% glycerol) using a French press. The lysate was centrifuged for 30 min at

30 000g to remove cell debris, and the supernatant was incubated with Ni–NTA resin (Machery-Nagel) for 30 min. The resin was then washed with lysis buffer and the protein was eluted with elution buffer (300 mM NaCl, 50 mM Tris pH 8, 300 mM imidazole, 3 mM β-mercaptoethanol, 10% glycerol) at room temperature. The 8×His-SUMO solubilization tag was removed by recombinant yeast Ulp1 protease (1 h or overnight at 277 K). The protein was further purified by size-exclusion chromatography (SEC) on a HiLoad 16/600 Superdex 75 pg column (GE Healthcare) in SEC buffer (50 mM NaCl, 50 mM Tris pH 7.4) followed by anion-exchange chromatography on a HiTrap Q HP column (GE Healthcare; buffer A, 50 mM NaCl, 50 mM Tris pH 7.4; buffer B, 1 M NaCl, 50 mM Tris pH 7.4) both at 277 K. Fractions containing the protein of interest were pooled and the protein was concentrated to 20 mg ml<sup>-1</sup> (the concentration was determined using the absorbance at 280 nm measured using a NanoDrop 1000 spectrophotometer from Thermo Fisher Scientific), aliquoted, flash-frozen in liquid nitrogen and stored at 193 K for future use.

### 2.2. Crystallization and crystallographic analysis

To set up drops, wild-type STING was supplemented with 0.5 mM 3',3'-c-di-GMP and 10 mM EDTA. The protein crystals grew in sitting drops consisting of a 1:1 mixture of protein solution and well solution [0.2 M lithium sulfate, 20% (w/v) PEG 3350]. The crystals grew in approximately two weeks at 291 K. The crystals were cryoprotected in mother liquor supplemented with 20% (v/v) glycerol and were flash-cooled in liquid nitrogen. An X-ray data set was collected from a single cooled crystal using the home source. The data set was processed (integration and scaling) by XDS (Kabsch, 2010) as summarized in Table 1. The structure was solved by molecular replacement (MR) using Phaser (McCoy *et al.*, 2007) from the CCP4 package (Winn *et al.*, 2011). The structure of STING (PDB entry 4ksy) was used as a search model. The ligand was placed using Coot (Debrecezeni & Emsley, 2012) and the structure was further improved using PHENIX (xyz coordinates and real-space refinement with twinning fraction 50%

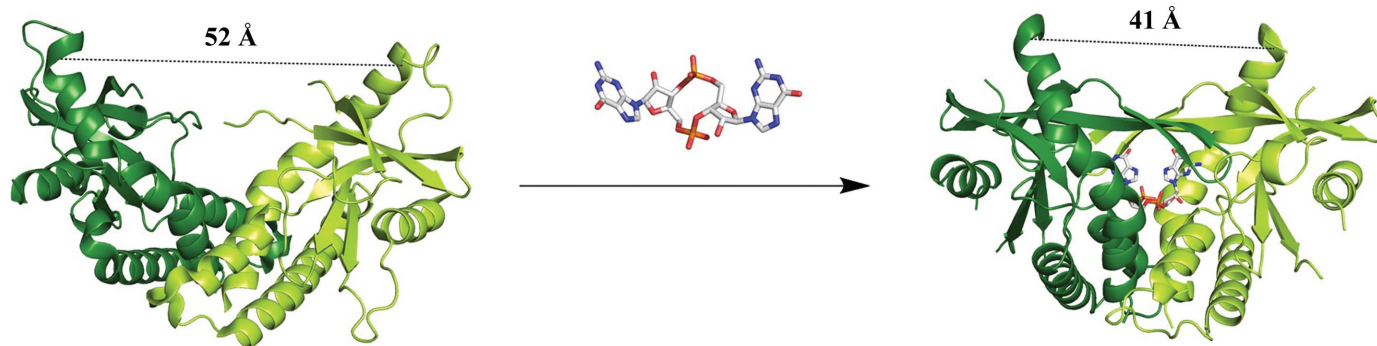


Figure 1

The closure of the ligand-binding domain of STING upon the binding of 3',3'-c-di-GMP. The monomers of the STING receptor cytosolic domain are coloured in shades of green, the C atoms of the ligand are grey and other atoms are coloured according to convention. The picture of STING in the open conformation is based on PDB entry 4emu and the picture of STING in the closed conformation is based on the structure presented in this study (PDB entry 6s86).

**Table 1**

Data collection and processing for STING in complex with 3',3'-c-di-GMP.

Values in parentheses are for the outer shell.

Diffraction source	Rigaku MicroMax-007 HF rotating anode
Wavelength (Å)	1.54187
Temperature (K)	100
Detector	Dectris PILATUS 200K
Crystal-to-detector distance (mm)	60
Rotation range per image (°)	0.1
Total rotation range (°)	180
Exposure time per image (s)	10
Space group	$P4_1$
$a, b, c$ (Å)	110.69, 110.69, 34.33
$\alpha, \beta, \gamma$ (°)	90, 90, 90
Resolution range (Å)	39.14–2.60 (2.693–2.600)
Total No. of reflections	85649 (9136)
No. of unique reflections	13223 (1325)
Completeness (%)	99.76 (100)
Multiplicity	6.5 (6.9)
$CC_{1/2}$	0.998 (0.82)
$\langle I/\sigma(I) \rangle$	17.72 (2.79)
$R_{\text{r.i.m.}}^\dagger$	7.60 (51.67)
Overall $B$ factor from Wilson plot (Å <sup>2</sup> )	56.92

<sup>†</sup> The  $R_{\text{r.i.m.}}$  value was estimated by multiplying the conventional  $R_{\text{merge}}$  value by the factor  $[N/(N-1)]^{1/2}$ , where  $N$  is the data multiplicity.

for  $h, -k, -l$ ; Adams *et al.*, 2010). The final statistics are summarized in Table 2. Structural figures were generated by *PyMOL* v.1.3r1 (Schrödinger). The structure was deposited in the Protein Data Bank (<https://www.rcsb.org/>) with accession code 6s86.

### 2.3. *In vitro* thermal stability assay

The ligands were dissolved in water and mixed with protein in TSA buffer (150 mM NaCl, 50 mM Tris pH 7.4). The final concentrations of the ligand and protein were 150 and 5  $\mu\text{M}$ , respectively. Alternatively, the TSA buffer also contained 10 mM  $\text{MgCl}_2$  or 100 mM EDTA. The mixtures were incubated on ice for 15 min. SYPRO Orange Protein Gel Stain (Sigma–Aldrich) was subsequently added (final 5 $\times$  concentration) and the mixtures were again incubated on ice for a further 15 min. The protein melting curves were measured using a LightCycler 480 Instrument II and the data were analysed using the *LightCycler* 480 software.

## 3. Results and discussion

### 3.1. Magnesium does not stabilize the CDN–STING complex

When we first started to grow STING crystals with various ligands, we supplemented the protein with 2 mM magnesium ion based on the first crystal structure of STING and the 'common' knowledge that phosphate groups bind to proteins via magnesium ions. However, we often observed crystals in conditions containing chelating agents such as 100 mM citrate buffer. Therefore, we decided to elucidate the role of magnesium more closely. We employed differential scanning fluorimetry, a method that can measure the melting temperature ( $T_m$ ) of a protein in various conditions (ligand concentration, buffer composition, presence of chelating

**Table 2**

Structure solution and refinement for STING in complex with 3',3'-c-di-GMP.

Values in parentheses are for the outer shell.

Final $R_{\text{work}}$ (%)	21.0 (28.5)
Final $R_{\text{free}}$ (%)	24.7 (31.8)
No. of non-H atoms	
Total	2741
Protein	2669
Ligand	46
Water	26
R.m.s. deviations	
Bonds (Å)	0.007
Angles (°)	0.96
Average $B$ factors (Å <sup>2</sup> )	
Overall	56.92
Protein	57.29
Ligands	40.99
Solvent	47.43
Ramachandran plot	
Most favoured (%)	97.26
Outliers (%)	0

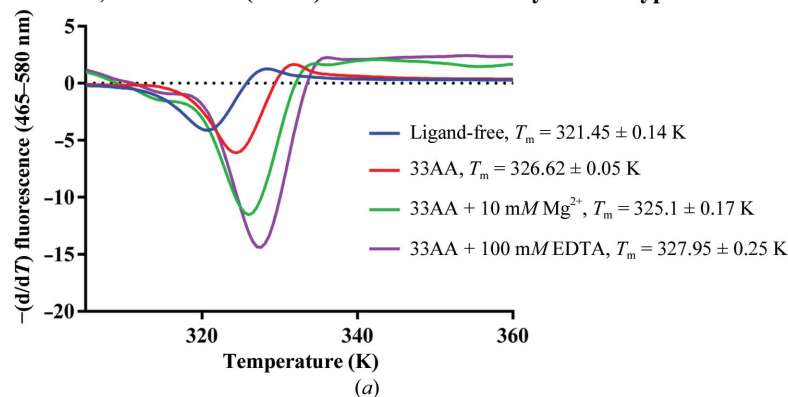
agents *etc.*). As expected, the  $T_m$  of STING was dependent on the presence of ligand and additives (Fig. 2). In the case of 3',3'-c-di-AMP [Fig. 2(a)], the change in melting temperature ( $\Delta T_m$ ) of the protein with and without ligand was approximately 5.2 K. Surprisingly, the presence of magnesium ions (at 10 mM) led to significant destabilization of the protein–ligand complex, with the  $T_m$  decreasing by 1.5 K to 325.1 K, contrary to what would be expected if magnesium were participating in the binding. However, the  $T_m$  still remained significantly higher compared with the unliganded protein ( $T_m = 321.45 \pm 0.14$  K). Addition of the chelating agent EDTA (100 mM) to the protein–ligand mixture led to an improvement in the stability of the complex ( $T_m = 327.95 \pm 0.25$  K), suggesting that even small concentrations of divalent cations that are perhaps bound to the protein during purification interfere with the ligand binding.

Next, we characterized the role of magnesium in the binding of another well known STING ligand, 3',3'-c-di-GMP [Fig. 2(b)]. In this case, the differences between the  $T_m$  values of the protein–ligand complex alone and in the presence of magnesium ions or EDTA were not significant. However, these results also argue that there is no need for magnesium in the binding site of STING, because its presence would increase the stability of the protein–ligand complex and EDTA would decrease it in the case in which magnesium was participating in the binding of the CDNs to STING. Instead, we observed no significant difference. In conclusion, magnesium ions do not stabilize the STING–3',3'-c-di-GMP complex and even destabilize the STING–3',3'-c-di-AMP complex. This was also indirectly confirmed by our crystallization trials: when comparing the quality of the crystals (shape, size, cryoprotection and diffraction limit) the best crystals were grown in the presence of EDTA.

### 3.2. The structure of the STING–3',3'-c-di-GMP complex

To further confirm that magnesium is not present in the STING–ligand complex, we grew crystals of the

**Influence of 3',3'-c-di-AMP (33AA) the thermal stability of wild-type STING**



**Influence of 3',3'-c-di-GMP (33GG) the thermal stability of wild-type STING**

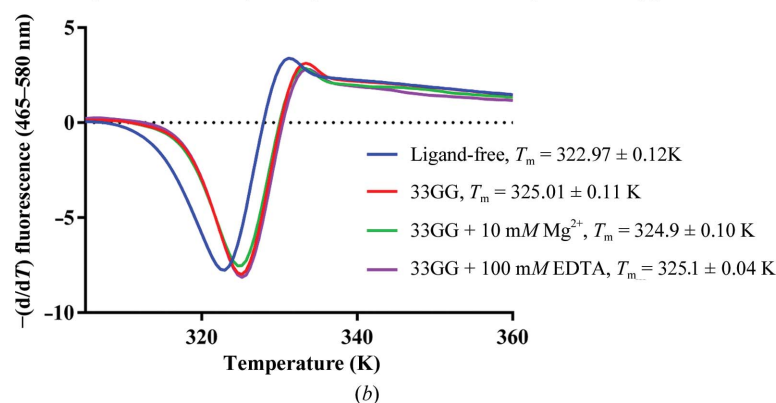


**Figure 2**

EDTA stabilizes the CDN–STING complex when magnesium is present. Representative melting curve of ligand-free STING and melting curves of the same protein in complex with 3',3'-c-di-AMP (a) or 3',3'-c-di-GMP (b) alone and with Mg<sup>2+</sup> or EDTA as an additive are shown. Three independent measurements were performed for each ligand.

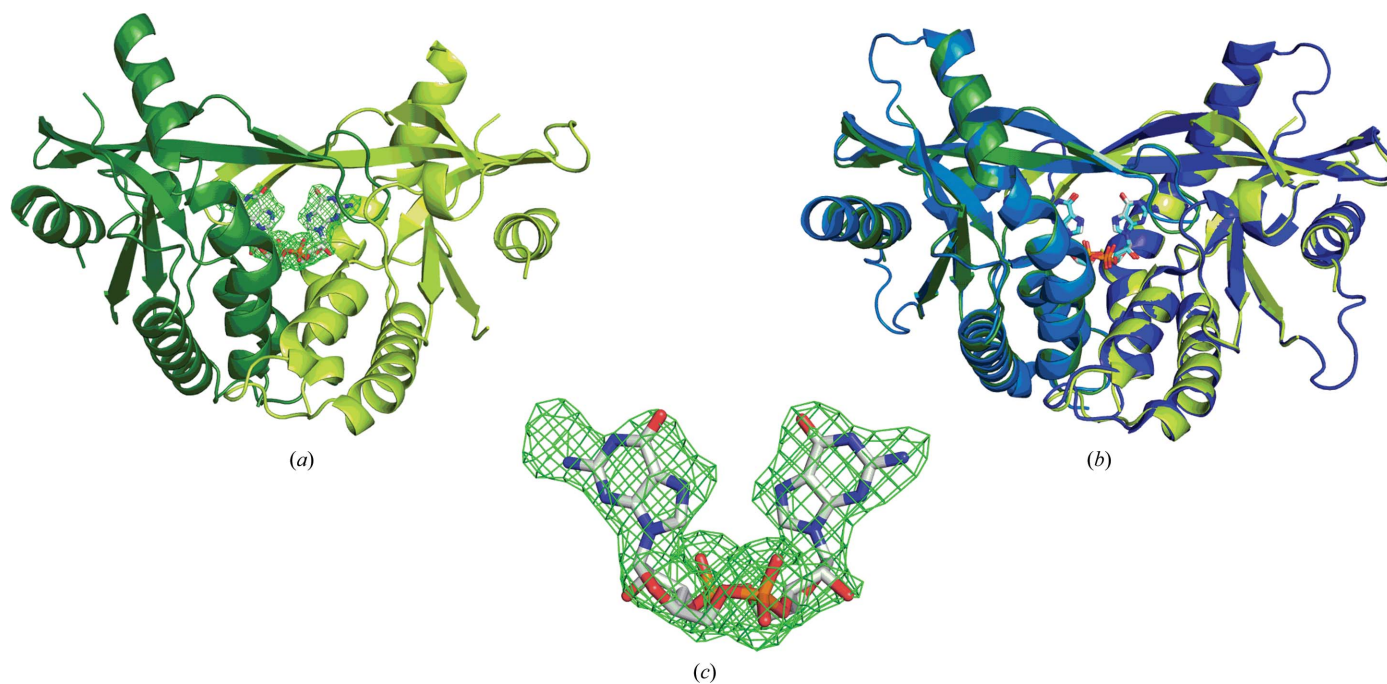


**Figure 3**

New structure of STING in complex with 3',3'-c-di-GMP and its comparison with PDB entry 4f5d. (a) Our structure of STING in complex with 3',3'-c-di-GMP (PDB entry 6rm0); the  $F_o - F_c$  map is contoured at  $2\sigma$ . (b) Alignment of our structure of STING (PDB entry 6rm0, green) and the structure solved by Huang and coworkers (PDB entry 4f5d, blue; Huang *et al.*, 2012); the r.m.s.d. on C $^\alpha$  atoms is 0.6163 Å. (c) Detailed view of the ligand in the  $F_o - F_c$  map contoured at  $2\sigma$ .

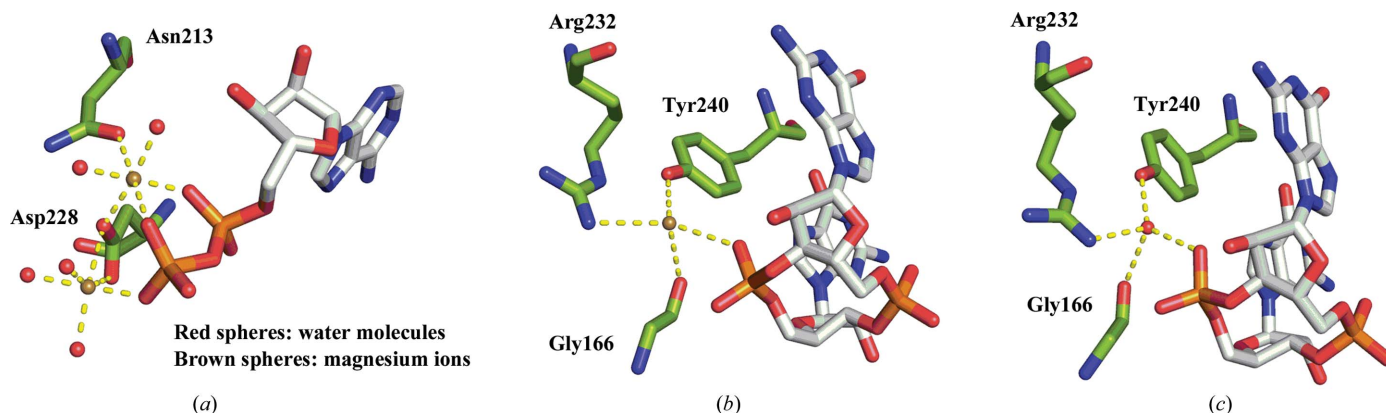


Figure 4

Magnesium versus water in the active site. (a) ADP is bound to *N*-acetylhexosamine 1-kinase via Mg atoms; the coordination bonds are arranged in an octahedral manner (PDB entry 4wh2). (b) Incorrect interpretation of the interaction of STING and 3',3'-c-di-GMP via an Mg atom (PDB entry 4f5d). (c) Binding of 3',3'-c-di-GMP in the active site of STING via a water molecule. For clarity, only amino-acid residues that interact with the ligands are shown. Colours of atoms are as follows: carbons in the protein, green; carbons in the ligand, grey; oxygen, red; nitrogen, blue; magnesium, brown. Bonds are shown as yellow dots.

STING–3',3'-c-di-GMP complex in the presence of 10 mM EDTA. We obtained crystals that diffracted to 2.6 Å resolution (as summarized in Table 1) at the home source and belonged to the tetragonal space group  $P4_1$ . The structure is virtually the same as the previous 3 Å resolution structure (Huang *et al.*, 2012) as long as only the positions of the C $^{\alpha}$  atoms (r.m.s.d. on C $^{\alpha}$  atoms of 0.6163 Å) and the ligand are considered (Fig. 3). However, how the ligand is held in the ligand-binding pocket is different (Fig. 4).

In an excellent publication entitled *Mg<sup>2+</sup> ions: do they bind to nucleobase nitrogens?* (Leonarski *et al.*, 2017) several structures with correctly or wrongly placed magnesium ions are described. Fig. 4(a) shows the typical binding mode of magnesium ions by the phosphate groups of ADP in complex with *N*-acetylhexosamine 1-kinase (Sato *et al.*, 2015). In this high-resolution structure (1.8 Å) magnesium ions are bound to their interaction partners by six coordination bonds, which must be always arranged in an octahedral molecular geometry. On the other hand, the magnesium ions placed in the structure of STING by Huang and coworkers [Fig. 4(b)] are involved in just four coordination bonds, which are arranged in the shape of a pyramid (Huang *et al.*, 2012). In addition, these coordination bonds are made with two hydrogen-bond donors and two hydrogen-bond acceptors, which is another sign of the presence of a water molecule at the given position. These facts indicate that an Mg atom was placed where a water molecule should have been. Our structure illustrates that water in fact mediates the interaction of Gly166, Arg232 and Tyr240 with the phosphate group of 3',3'-c-di-GMP.

In conclusion, the correct identification of ligands is far from trivial, especially in low-resolution structures, and knowledge of the chemistry may be necessary. In addition, for isoelectric ligands (Mg<sup>2+</sup> and the water molecule are those encountered most often in protein crystallography) high resolution in itself will not help without considering other factors such as proper geometry and the lengths of hydrogen and coordination bonds.

## Funding information

This work was supported by Gilead Sciences Inc. and by the European Regional Development Fund OP RDE Project 'Chemical biology for drugging undruggable targets (ChemBioDrug)' (No. CZ.02.1.01/0.0/0.0/16\_019/0000729). Support from the Academy of Sciences of the Czech Republic (RVO:61388963) is also acknowledged.

## References

- Adams, P. D., Afonine, P. V., Bunkóczi, G., Chen, V. B., Davis, I. W., Echols, N., Headd, J. J., Hung, L. W., Kapral, G. J., Grosse-Kunstleve, R. W., McCoy, A. J., Moriarty, N. W., Oeffner, R., Read, R. J., Richardson, D. C., Richardson, J. S., Terwilliger, T. C. & Zwart, P. H. (2010). *Acta Cryst.* **D66**, 213–221.
- Barber, G. N. (2015). *Nature Rev. Immunol.* **15**, 760–770.
- Boura, E., Rezabkova, L., Brynda, J., Obsilova, V. & Obsil, T. (2010). *Acta Cryst.* **D66**, 1351–1357.
- Chen, Q., Sun, L. & Chen, Z. J. (2016). *Nature Immunol.* **17**, 1142–1149.
- Corrales, L., Glickman, L. H., McWhirter, S. M., Kanne, D. B., Sivick, K. E., Katibah, G. E., Woo, S. R., Lemmens, E., Banda, T., Leong, J. J., Metchette, K., Dubensky, T. W. Jr & Gajewski, T. F. (2015). *Cell Rep.* **11**, 1018–1030.
- Debrecezeni, J. É. & Emsley, P. (2012). *Acta Cryst.* **D68**, 425–430.
- Fitzgerald, K. A., McWhirter, S. M., Faia, K. L., Rowe, D. C., Latz, E., Golenbock, D. T., Coyle, A. J., Liao, S. M. & Maniatis, T. (2003). *Nature Immunol.* **4**, 491–496.
- Fu, J., Kanne, D. B., Leong, M., Glickman, L. H., McWhirter, S. M., Lemmens, E., Mechette, K., Leong, J. J., Lauer, P., Liu, W., Sivick, K. E., Zeng, Q., Soares, K. C., Zheng, L., Portnoy, D. A., Woodward, J. J., Pardoll, D. M., Dubensky, T. W. Jr & Kim, Y. (2015). *Sci. Transl. Med.* **7**, 283ra52.
- Hercik, K., Brynda, J., Nencka, R. & Boura, E. (2017). *Arch. Virol.* **162**, 2091–2096.
- Huang, Y.-H., Liu, X.-Y., Du, X.-X., Jiang, Z.-F. & Su, X.-D. (2012). *Nature Struct. Mol. Biol.* **19**, 728–730.
- Kabsch, W. (2010). *Acta Cryst.* **D66**, 125–132.
- Leonarski, F., D'Ascenzo, L. & Auffinger, P. (2017). *Nucleic Acids Res.* **45**, 987–1004.
- McCoy, A. J., Grosse-Kunstleve, R. W., Adams, P. D., Winn, M. D., Storoni, L. C. & Read, R. J. (2007). *J. Appl. Cryst.* **40**, 658–674.

- Sato, M., Arakawa, T., Nam, Y.-W., Nishimoto, M., Kitaoka, M. & Fushinobu, S. (2015). *Biochim. Biophys. Acta*, **1854**, 333–340.
- Shang, G., Zhang, C., Chen, Z. J., Bai, X.-C. & Zhang, X. (2019). *Nature (London)*, **567**, 389–393.
- Shi, H., Wu, J., Chen, Z. J. & Chen, C. (2015). *Proc. Natl Acad. Sci. USA*, **112**, 8947–8952.
- Shu, C., Yi, G., Watts, T., Kao, C. C. & Li, P. (2012). *Nature Struct. Mol. Biol.* **19**, 722–724.
- Strzyz, P. (2019). *Nature Rev. Mol. Cell Biol.* **20**, 266.
- Winn, M. D., Ballard, C. C., Cowtan, K. D., Dodson, E. J., Emsley, P., Evans, P. R., Keegan, R. M., Krissinel, E. B., Leslie, A. G., McCoy, A., McNicholas, S. J., Murshudov, G. N., Pannu, N. S., Potterton, E. A., Powell, H. R., Read, R. J., Vagin, A. & Wilson, K. S. (2011). *Acta Cryst. D* **67**, 235–242.
- Yin, Q., Tian, Y., Kabaleeswaran, V., Jiang, X., Tu, D., Eck, M. J., Chen, Z. J. & Wu, H. (2012). *Mol. Cell*, **46**, 735–745.
- Zhang, C., Shang, G., Gui, X., Zhang, X., Bai, X.-C. & Chen, Z. J. (2019). *Nature (London)*, **567**, 394–398.
- Zhang, X., Shi, H. P., Wu, J. X., Zhang, X. W., Sun, L. J., Chen, C. & Chen, Z. J. (2013). *Mol. Cell*, **51**, 226–235.